Three-body correlations in liquid ^{4}He

Q. N. Usmani,* S. Fantoni,† and V. R. Pandharipande
Department of Physics and Materials Research Laboratory, University of Illinois at Urbana-Champaign, Urbana, Illinois 61801
(Received 10 May 1982)

We report results of variational calculations of liquid ^{4}He with wave functions containing optimized two-body and three-body correlations. The hypernetted-chain (HNC) summation method is used, and the elementary and Abe diagrams are calculated with the scaling approximation. Comparisons with the existing Monte Carlo calculations suggest that this HNC-scaling method is almost exact. The logarithm of the three-body correlation of f_{ijk} contains terms having $P_l(\hat{r}_{ij}\cdot\hat{r}_{ik})$, $l=0$, 1, and 2. As expected on theoretical grounds, the $l=1$ term of $\ln f_{ijk}$ dominates, while the $l=0$ and 2 terms give rather small changes in the binding energy. The f_{ijk} makes up $\sim 85\%$ of the difference between the Jastrow and presumably exact Green's-function Monte Carlo (GFMC) energies. The best variational energies obtained with the HFDHE2 potential of Aziz *et al.* are within $(2\pm 1)\%$ of the GFMC and experimental results. The liquid structure function $S(k)$ is also well explained by the variational wave function.

I. INTRODUCTION

The ground state of liquid ^{4}He has been the object of many calculations during the past two decades. These calculations start from a microscopic model of the interaction between two helium atoms, and attempt to explain the known zero-temperature equation of state $E(\rho)$, and the liquid structure function $S(k)$ at equilibrium density $\rho_0 = 0.3648\sigma^{-3}$. The numerical problem of solving the many-body Schrödinger equation for the ground state has been resolved, to a large extent, by the Green's-function Monte Carlo method[1] (GFMC). One of the results provided by GFMC calculations[2] is that the commonly used Lennard-Jones (6-12) potential does not give a realistic description of the He-He interaction in the liquid phase. A better candidate seems to be the HFDHE2 potential suggested by Aziz *et al.*[3]

A quantitative understanding of the structure of the ground-state wave function still remains an open and interesting problem. An analytic ground-state wave function would be particularly useful to extend the microscopic theory to treat the elementary excitations[4] and finite-temperature properties of helium liquids. A successful approach in this direction has been provided by the variational theory.

The ground-state energies obtained with the simple Jastrow wave function[5,6]

$$\Psi_J = \prod_{i<j} f_{ij} \tag{1.1}$$

are too high, and the peak of $S(k)$ is too broad, as compared to experiment or the GFMC results. Thus this wave function does not provide an adequate description of the ground state. Calculations performed with Feenberg's correlated-basis perturbation theory[7] as well as variational calculations[8,9] indicate that three-body correlations account for much of the difference between the Jastrow and GFMC ground-state $E(\rho)$.

The most reliable Monte Carlo calculations[9] use a three-body correlation:

$$f_{ijk} = \exp(-\tfrac{1}{2}q_{ijk}) , \tag{1.2}$$

$$q_{ijk} = \sum_{\text{cyc}} \xi_1(r_{ij})\xi_1(r_{ik})P_1(\hat{r}_{ij}\cdot\hat{r}_{ik}) , \tag{1.3}$$

in the variational wave function

$$\Psi = \prod_{i<j} f_{ij} \prod_{i<j<k} f_{ijk} . \tag{1.4}$$

Here $\sum_{\text{cyc}}$ represents a sum of the three terms obtained by replacing ijk with jki and kij, and $\hat{r}_{ij}$ are unit vectors. The form of this three-body correlation, suggested in Ref. 8, takes into account the Feynman-Cohen[10] backflow in the ground state. The equilibrium density obtained with this wave function,[9] with the Lennard-Jones (LJ) potential, is the experimental (and GFMC) equilibrium density ρ_0. The calculated $E(\rho_0)$ is -6.55 K against the Jastrow, GFMC, and experimental values of -5.94, -6.85, and -7.14 K, respectively. Thus the f_{ijk} of

Ref. 9 appears to make up $\sim\frac{2}{3}$ of the difference between the Jastrow and presumably exact GFMC results.

The object of this work is to make a systematic search for three-body correlations, and examine the extent to which the wave function (1.4) can explain the GFMC and experimental results. To minimize the uncertainties due to a poor two-body correlation we use optimized f_{ij}. The GFMC $E(\rho_0)$ with the HFDHE2 potential is -7.12 ± 0.02 K, while the energy obtained with the optimized Jastrow wave function is -5.94 K. It is found that the q_{ijk} given by Eq. (1.3) can lower it down to -6.81 K. It is possible to lower it further to -6.96 ± 0.05 K by generalizing the q_{ijk} to

$$q_{ijk}=\sum_{\text{cyc}}\sum_{l=0,2}\xi_l(r_{ij})\xi_l(r_{ik})P_l(\hat{r}_{ij}\cdot\hat{r}_{ik})\ . \tag{1.5}$$

The $l=0$ term of q_{ijk} lowers $E(\rho_0)$ by 0.12 K, while the $l=2$ term lowers it by only 0.03 K. The $S(k)$ obtained with the "best" f_{ijk} is in excellent agreement with the experimental and GFMC results. We thus find that wave functions of type (1.4) give a very accurate, though not exact, description of the liquid-^{4}He ground state.

The hypernetted-chain-summation (HNC/S) method is used to calculate expectation values with the wave function (1.4). The contribution of elementary diagrams formed with $g-1$ links, where $g(r)$ is the pair distribution function, is summed to all orders in the expansion with the scaling approximation.[11] The four-body elementary diagrams having f_{ijk}^2-1 links are also calculated. The Monte Carlo results of Ref. 9 are reproduced within 0.05 K to ascertain the accuracy of this method. Formal expressions for the energy and distribution functions are given in Sec. II, while the HNC/S calculation is outlined in Sec. III. The results are given in Sec. IV.

II. FORMALISM

Two (or more) formally equivalent expressions can be obtained for the expectation value of the energy with wave function (1.4), by integrating the kinetic energy terms by parts. The so-called Jackson-Feenberg[12] energy $E_{\rm JF}$ is given by

$$E_{\rm JF}=\tfrac{1}{2}\rho\int d^3r_{ij}g_{ij}\left\{v_{ij}-\frac{\hbar^2}{2m}\left[\frac{\nabla^2 f_{ij}}{f_{ij}}-\left[\frac{\nabla f_{ij}}{f_{ij}}\right]^2\right]\right\}+\frac{\hbar^2}{16m}\rho^2\int d^3r_{ij}d^3r_{ik}g_{3,ijk}\nabla_i^2 q_{ijk}\ , \tag{2.1}$$

and the "Pandharipande-Bethe" energy[13] $E_{\rm PB}$ is

$$E_{\rm PB}=\tfrac{1}{2}\rho\int d^2r_{ij}g_{ij}\left[v_{ij}-\frac{\hbar^2}{m}\frac{\nabla^2 f_{ij}}{f_{ij}}\right]$$
$$-\frac{\hbar^2}{2m}\rho^2\int d^3r_{ij}d^3r_{ik}g_{3,ijk}\left[\frac{\nabla_i f_{ij}\cdot\nabla_i f_{ik}}{f_{ij}f_{ik}}+\frac{1}{2}\frac{\nabla_i^2 f_{ijk}}{f_{ijk}}+2\frac{\nabla_i f_{ij}\cdot\nabla_i f_{ijk}}{f_{ij}f_{ijk}}\right]-T_4-T_5\ , \tag{2.2}$$

$$T_4=-\frac{\hbar^2}{2m}\rho^3\int d^3r_{ij}d^3r_{ik}d^3r_{il}g_{4,ijkl}\left[\frac{\nabla_i f_{ij}\cdot\nabla_i f_{ikl}}{f_{ij}f_{ikl}}+\frac{\nabla_i f_{ijk}\cdot\nabla_i f_{ikl}}{f_{ijk}f_{ikl}}\right], \tag{2.3}$$

$$T_5=-\frac{\hbar^2}{8m}\rho^4\int d^3r_{ij}d^3r_{ik}d^3r_{il}d^3r_{im}\,g_{5,ijklm}\frac{\nabla_i f_{ijk}\cdot\nabla_i f_{ilm}}{f_{ijk}f_{ilm}}\ . \tag{2.4}$$

The g_{ij}, $g_{3,ijk}$, $g_{4,ijkl}$, and $g_{5,ijklm}$ are two-, three-, four-, and five-body distribution functions. The two-body g_{ij} is given by[8]

$$g_{ij}=f_{ij}^2\exp(N_{ij}+C_{ij}+\epsilon_{ij})\ , \tag{2.5}$$

where N_{ij} is the contribution of nodal diagrams,

$$N_{ij}=\rho\int d^3r_{ij}(g_{ik}-1)(g_{jk}-1-N_{jk})\ , \tag{2.6}$$

C_{ij} is the dressed three-body link,

$$C_{ij}=\rho\int d^3r_{ik}(f_{ijk}^2-1)g_{ik}g_{jk}\ , \tag{2.7}$$

and ϵ_{ij} is the sum of all elementary diagrams. The three-body distribution function is given by

$$g_{3,ijk}=g_{ij}g_{jk}g_{ki}f_{ijk}^2\exp(A_{ijk})\ , \tag{2.8}$$

where A_{ijk} is the sum of the Abe diagrams.[14] It is simple to write expressions for four- and five-body distribution functions, but they are hard to calculate.

The main problem in the application of this

chain-summation method has always been the calculation of ϵ_{ij} and A_{ijk}. In the HNC approximation both A_{ijk} and ϵ_{ij} are neglected. We may order the elementary and Abe diagrams according to the number of points $n \geq 4$:

$$\epsilon_{ij} = \epsilon_{4,ij} + \epsilon_{5,ij} + \cdots , \tag{2.9}$$

$$A_{ijk} = A_{4,ijk} + A_{5,ijk} + \cdots . \tag{2.10}$$

In an HNC/n calculation the sums (2.9) and (2.10) are truncated at the nth term. Unfortunately it is known[15] that (2.9) is not a rapidly converging series. In the absence of a three-body correlation the $\epsilon_{n>4}$ ($A_{n>4}$) are approximately proportional to ϵ_4 (A_4), and in the HNC/S method this property is used to sum the series (2.9) and (2.10) to all orders.

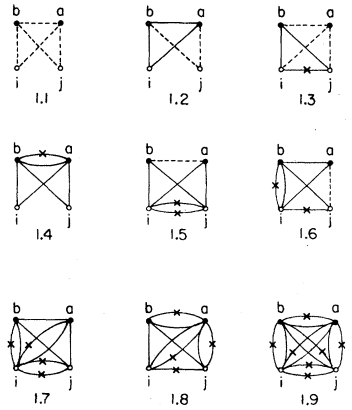

FIG. 1. $n=4$ elementary diagrams. The $\epsilon^g_{4,ij}$ is given by diagram 1.1, while 1.2—1.9 contribute to $\epsilon^t_{4,ij}$. The dashed lines represent $g-1$ links, while the triangles denote three-body correlations as discussed in the text.

III. THE CALCULATION

The elementary and Abe diagrams are separated into two parts:

$$\epsilon_{ij} = \epsilon^g_{ij} + \epsilon^t_{ij} = \sum_{n\geq 4} \epsilon^g_{n,ij} + \epsilon^t_{ij} , \tag{3.1}$$

$$A_{ijk} = A^g_{ijk} + A^t_{ijk} = \sum_{n\geq 4} A^g_{n,ijk} + A^t_{ijk} . \tag{3.2}$$

The ϵ^g_n and A^g_n contain all the diagrams that have only $(g-1)$ links, while ϵ^t and A^t diagrams must have at least one explicit three-body correlation. In the absence of three-body correlations (i.e., when $f_{ijk}=1$) the ϵ^t and A^t are zero, and ϵ and A are given by ϵ^g and A^g. The f_{ijk} has an implicit effect on the ϵ^g and A^g via its influence on the pair distribution function g.

The four-body elementary and Abe diagrams are shown in Figs. 1 and 2, where the following notation is used. The solid dots and open circles represent the positions of internal and external points, respectively. The $\epsilon_{n,ij}$ ($A_{n,ijk}$) diagrams have two (three) external points i,j (i,j,k) and $n-2$ ($n-3$) internal points. The dashed lines joining points a and b represent $g_{ab}-1$, while a triangle joining a, b, and c represents

$$g_{ab}g_{bc}g_{ca}(f^2_{abc}-1) .$$

A cross on the ab side of the triangle indicates that the factor g_{ab} should be omitted. Thus the triangle i,j,b of diagram 1.3 represents

$$g_{ib}g_{jb}(f^2_{ijb}-1) .$$

The crosses are needed to ascertain that the diagrams do not contain squares or higher powers of g_{ab}, and the g's between external points. The contribution of the diagram is obtained by integrating over all internal points with appropriate symmetry and density factors. Thus, for example, we have

$$\epsilon^t_{ij}\ (\text{diagram } 1.6) = \rho^2 \int (f^2_{ijb}-1)(f^2_{iba}-1) g_{ib}g_{jb}g_{ia}g_{ba}(g_{ja}-1) d^3r_a d^3r_b , \tag{3.3}$$

$$A^t_{ijk}\ (\text{diagram } 2.4) = \rho \int (f^2_{jkb}-1) g_{jb}g_{kb}(g_{ib}-1) d^3r_b . \tag{3.4}$$

The HNC/S method is ideally suited for calculating the expectation values with wave functions (1.1). In this case the $f_{ijk}=1$ and the terms T_4 and T_5 of $E_{\rm PB}$ [Eq. (2.2)] are zero. Thus the $E_{\rm PB}$ depends only upon g_{ij} and $g_{3,ijk}$, while $E_{\rm JF}$ depends only on g_{ij}. Both these energies can be calculated when ϵ_{ij} and A_{ijk} are known. However, in general $E_{\rm PB} \neq E_{\rm JF}$ if the series (2.9) and (2.10) for ϵ and A are truncated. The HNC/S method makes an apparently "accurate" assumption:

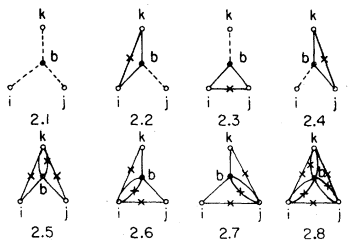

FIG. 2. $n=4$ Abe diagrams. The $A^g_{4,ijk}$ is given by diagram 2.1, while 2.2—2.8 contribute to $A^t_{4,ijk}$.

$$\epsilon_{ij}=\epsilon^g_{ij}=(1+s)\epsilon^g_{4,ij}\ , \tag{3.5}$$

$$A_{ijk}=A^g_{ijk}=(1+s/2)A^g_{4,ijk}\ , \tag{3.6}$$

and uses $E_{\rm PB}=E_{\rm JF}$ to determine the scaling factor s.

In this work the $f_{ijk}\neq 1$ and ϵ^t and $A^t\neq 0$. However, the $g_{ij}-1$ is not much affected by the f_{ijk}, and so we expect the scaling approximation to be valid for the ϵ^g and A^g. The ϵ_{ij} and A_{ijk} are approximated as follows:

$$\epsilon_{ij}=(1+s)\epsilon^g_{4,ij}+\epsilon^t_{4,ij}\ , \tag{3.7}$$

$$A_{ijk}=(1+s/2)A^g_{4,ijk}+A^t_{4,ijk}\ . \tag{3.8}$$

These equations should be valid when the three-body correlations are small, or when the series for ϵ^t and A^t are rapidly convergent.

We further note that the f_{ijk} have a very small effect on the two-body distribution function g_{ij}, as shown in Fig. 3. Thus it is very reasonable to assume that the value of s is unaffected by the three-body correlations. This allows the s to be determined by setting $f_{ijk}=1$ and equating $E_{\rm PB}$ with $E_{\rm JF}$. The energy with the wave function containing f_{ijk} is calculated with the Jackson-Feenberg expression (2.1) that has only g_{ij} and $g_{3,ijk}$ terms. The g_{ij} and $g_{3,ijk}$ are obtained from Eqs. (2.5)–(2.8) and (3.7) and (3.8), and the problem of calculating the $g_{4,ijkl}$ and $g_{5,ijklm}$ in the $E_{\rm PB}$ is avoided.

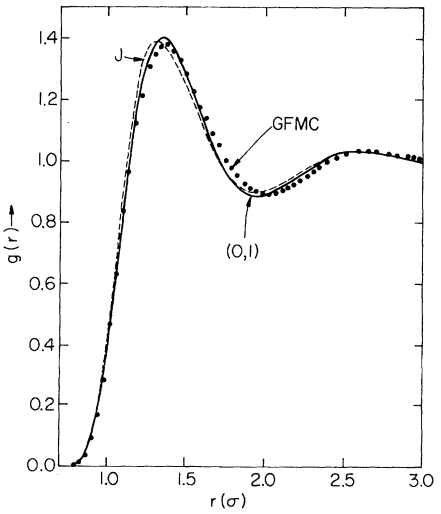

FIG. 3. Pair distribution functions obtained at $\rho=0.365\sigma^{-3}$ in Jastrow ($f_{ijk}=1$) and $l=0,1$ (q_{ijk} [Eq. (1.5)] containing $l=0$ and 1 correlations) calculations are shown by dashed and solid lines, respectively. The dots are from GFMC calculations.

In order to compare our results with the presumably exact variational Monte Carlo results we have calculated the $E(\rho)$ and g_{ij} in the Lennard-Jones (6,12) model of liquid ^{4}He with the wave function of Ref. 9. Here the two-body correlation has the McMillan form,

$$f_{ij}=\exp[-\tfrac{1}{2}(b/r)^5]\ , \tag{3.9}$$

the three-body q_{ijk} contains only the $l=1$ term, and the $\xi_1(r)$ is given by

$$\xi_1(r)=\begin{cases}\sqrt{\lambda}r\exp\left[-\left[\dfrac{r-r_{tl}}{w_1}\right]^2\right]\left[\dfrac{r-r_B}{r_B}\right]^3 \\ \qquad\qquad\qquad\qquad \text{for } r<r_B\ , \\ 0 \quad \text{for } r>r_B\ .\end{cases} \tag{3.10}$$

The values of the parameters b, λ, r_{tl}, and w_1 are given in Ref. 9, and $r_B=\frac{1}{2}(108/\rho)^{1/3}$ is half the size of the simulation cube used in the Monte Carlo calculation. The results of our HNC/S calculations for $E(\rho)$ and $g(r)$ are compared with the Monte Carlo (MC) results[9] in Tables I and II, respectively. These suggest that the approximations (3.7) and (3.8) for ϵ and A are quite accurate.

We now discuss, in some detail, the approximations (3.7) and (3.8) and their implications on our calculations. The first row of Table III gives the energy in the HNC approximation, i.e., when $\epsilon=A=0$. Taking $\epsilon=\epsilon^g_4$ and $A=A^g_4$ lowers the energy by 0.48 K (the difference of the energies of the first two rows). When all the elementary diagrams having only $g-1$ bonds are summed up with the scaling approximation, the energy further lowers to -5.82 K (third row). On adding ϵ^t_4 and A^t_4 the energy goes down by 0.67 to -6.49 K which is close to the MC value -6.53 K. The effect of ϵ^t_4 and A^t_4 on the energy is quite sizable and is half that of ϵ^g_4 and A^g_4. However, the excellent agreement between the present and the MC results indicates that $\epsilon^t_{n\geq 5}$ and $A^t_{n\geq 5}$ do not have an appreciable contribution. Either the series for ϵ^t and A^t are rapidly convergent or the $\epsilon^t_{n\geq 5}$ and $A^t_{n\geq 5}$ contributions cancel to a large extent.

TABLE I. The $E(\rho)$ of liquid ^{4}He with LJ potential.

ρ (σ^{-3})	E (MC)	E (HNC/S)	s
0.333	−6.46	−6.42	2.50
0.365	−6.53	−6.49	2.72
0.401	−6.37	−6.34	3.08

TABLE II. The properties of $g(r)$ with the LJ model at $\rho=\rho_0$. The $r_{\max 1}$, $r_{\min 1}$, and $r_{\max 2}$ give the locations of the first maximum, minimum, and second maximum of $g(r)$ in units of $\sigma=2.556$ Å; the values of $g(r)$ at these points are given by $g_{\max 1}$, $g_{\min 1}$, and $g_{\max 2}$.

	$r_{\max 1}$	$g_{\max 1}$	$r_{\min 1}$	$g_{\min 1}$	$r_{\max 2}$	$g_{\max 2}$
HNC/S	1.35	1.302	2.01	0.915	2.68	1.027
MC	1.35 ±0.02	1.300 ±0.005	2.03 ±0.02	0.915 ±0.003	2.68 ±0.02	1.030 ±0.005

In Fig. 4 we have plotted the important contributions to ϵ_4^t. We note that diagrams having two explicit three-body correlations, such as 1.4, 1.5, and 1.6, have contributions comparable to those of 1.2 and 1.3 which have only one explicit three-body correlation. Thus it appears that expanding the ϵ^t and A^t in the number of explicit (f_{ijk}^2-1) factors may not be useful.

It should be pointed out here that, because of the box cutoff, the $\xi_1(r)$ used in the Monte Carlo calculations[9] is very sharp. In this work we do not need to impose this cutoff. The $\xi_1(r)$ obtained in limit $r_B\to\infty$ is weaker and more smooth. The A_4^t and ϵ_4^t obtained with the present f_{ijk} are smaller, and so are their contributions to the energy (Table III).

IV. RESULTS AND DISCUSSION

In this section we present the results obtained for the ground state of liquid ^{4}He with the HFDHE2 potential suggested by Alrichs *et al.*,[16] with the parameters determined by Aziz *et al.*[3] by fitting the result of Hartree-Fock calculations of McLaughlin and Schoefer,[17] the second virial coefficient and the thermal conductivity data. Extensive calculations show that this potential is the most realistic in predicting several experimental two-body measurements,[3] and the energy[2] of liquid ^{4}He.

The two-body correlation function $f(r)$ used in the calculations are obtained following the optimization procedure described in Ref. 11. The three-body correlation function f_{ijk} has been taken of the form given in Eq. (1.5). Since the $l=1$ term is expected to be the main term of the q_{ijk}, a detailed variational calculation has been carried out keeping only the $l=1$ component in q_{ijk}. The $\xi_1(r)$ is taken to be of the form

$$\xi_1(r)=\sqrt{\lambda_1}r\exp\left[-\left[\frac{r-r_{t1}}{\omega_1}\right]^2\right]. \tag{4.1}$$

The dependence of the variational parameters λ_1, r_{t1}, and ω_1 on the density is very weak and is neglected in this work. Letting λ_1, r_{t1}, and ω_1 depend on ρ leads to changes in the energy that are within the accuracy of the calculation. The optimum values of the parameters are given in Table IV. It should be noted that the trial function (4.1) is variationally preferred over that of Eq. (3.10); the r_B term raises the energy. The calculated energies are listed in Table V, where the Jastrow energy is also reported. For sake of comparison we have computed the energy at density ρ_0 by using the trial function $f(r)$ and $\xi_1(r)$ as given by Eqs. (3.9) and (3.10), with the following values of the parameters: $b=1.21\sigma$, $\lambda_1=-14$, $r_{t1}=0.82$, $\omega_1=0.50$, $r_{B_1}=3.00\sigma$. Our result of -6.65 K compares very

TABLE III. The $E(\rho_0)$ of liquid ^{4}He with LJ potential. The columns MC and Present, respectively, give energies obtained with the $\xi_1(r)$ used in Monte Carlo (Ref. 9) and the present work.

Approximations			E (K)	
ϵ_4^g	scaling	ϵ_4^t	MC f_{ijk}	Present f_{ijk}
No	No	No	−4.13	−4.60
Yes	No	No	−4.61	−5.02
Yes	Yes	No	−5.82	−6.21
Yes	Yes	Yes	−6.49	−6.49
	Monte Carlo result		−6.53	

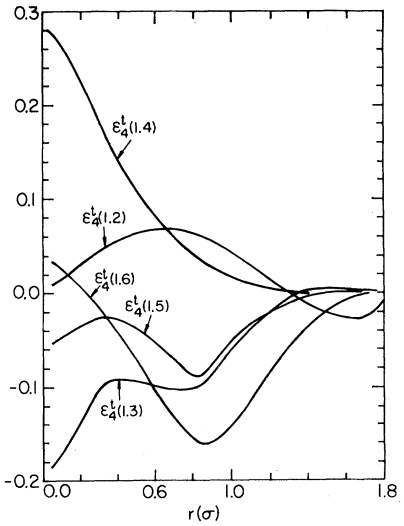

FIG. 4. Contributions of the important $\epsilon^t_{4,ij}$ diagrams plotted as a function of r.

well with the -6.72 K obtained[18] with the MC method, but it is above the -6.81 K obtained with optimized f_{ij} and $\xi_1(r)$ given by Eq. (4.1).

The energy has been further minimized including the $l=0$ and 2 components in q_{ijk}. The trial functions $\xi_0(r)$ and $\xi_2(r)$ have been taken of the form

$$\xi_0(r)=\sqrt{\lambda_0}(r-r_{t0})\exp\left[-\left[\frac{r-r_{t0}}{\omega_0}\right]^2\right], \tag{4.2}$$

$$\xi_2(r)=\sqrt{\lambda_2}r\exp\left[-\left[\frac{r-r_{t2}}{\omega_2}\right]^2\right]. \tag{4.3}$$

TABLE IV. The variational parameters of q_{ijk}.

l	λ_l	$r_{tl(\sigma)}$	$\omega_{l(\sigma)}$
0	-0.044	1.1	0.65
1	-1.08	0.80	0.41
2	0.05	0.85	0.45

The velocity of sound $c(\rho)$ obtained from the $l=0,1$ variational energies are reported in Table VI along with the experimental and GFMC values.[19–21] These results have been obtained by fitting the calculated $E(\rho)$ with a third-degree polynomial,

$$E(\rho)=E_0+B\left[\frac{\rho-\rho_0}{\rho_0}\right]^2+C\left[\frac{\rho-\rho_0}{\rho_0}\right]^3. \tag{4.4}$$

TABLE V. The calculated energies [E (var)] of liquid ^{4}He in K compared with the GFMC and experimental energies. The second column gives the wave function used in the calculation. In this column J indicates Jastrow, 1 indicates q_{ijk} with P_1 term only, 0,1 indicates q_{ijk} with P_0 and P_1 terms, etc.

ρ (σ^{-3})	Ψ	s	$\langle T\rangle$	$\langle V\rangle$	E (var)	E (GFMC)	E (Expt.)
0.328	J	2.18	12.64	-18.76	-6.12		
	1		12.38	-19.13	-6.75	-7.03	
						±0.04	
	0,1		12.26	-19.06	-6.80		
0.347	J	2.23	13.96	-20.00	-6.04		
	1		13.66	-20.43	-6.77		
	0,1		13.40	-20.23	-6.83		
0.365	J	2.44	15.25	-21.29	-5.94		
	1		14.91	-21.72	-6.81	-7.12	-7.14
	0,1		14.72	-21.65	-6.93	±0.02	
	0,1,2		14.77	-21.73	-6.96		
0.401	J	2.78	18.12	-23.58	-5.46		
	1		17.53	-24.18	-6.65	-6.89	-7.00
	0,1		17.45	-24.17	-6.72	±0.05	
	0,1,2		17.50	-24.26	-6.76		
0.438	J	3.12	21.35	-26.07	-4.72		
	1		20.53	-26.76	-6.23	-6.56	-6.53
						±0.06	
	0,1		20.34	-26.77	-6.43		

TABLE VI. Sound velocities in m/sec. The GFMC sound velocities are calculated with the parameters $E_0=-7.110$ K, $\rho_0=0.3600\sigma^{-3}$, $B=10.08$ K, and $C=12.59$ K of Ref. 2.

ρ (σ^{-3})	HNC/S	GFMC	Expt.
0.365	235	215	238.2
0.401	314	294	306.2
0.438	396	377	375.2

The values obtained with this fit are

$$E_0=-6.892,\quad B=12.72\text{ K},$$
$$\rho_0=0.3624,\quad C=12.16\text{ K}. \tag{4.5}$$

The experimental E_0 and ρ_0 are -7.14 K and $0.3648\sigma^{-3}$, respectively. The variational and GFMC $E(\rho)$ are compared in Fig. 5, while the static structure functions

$$S(k)=1+\rho\int d^3r[g(r)-1]e^{i\vec{k}\cdot\vec{r}} \tag{4.6}$$

are compared in Fig. 6.

The wave function (1.4) does very well in reproducing the GFMC energies and distribution function. The f_{ijk} makes up $\sim 85\%$ of the difference between the Jastrow and GFMC $E(\rho)$. The HNC/S calculation generally underestimates the variational energies (Table I) by ~ 0.05 K, and so a more accurate calculation of the energy expectation value would presumably reduce the difference between the variational and GFMC results.

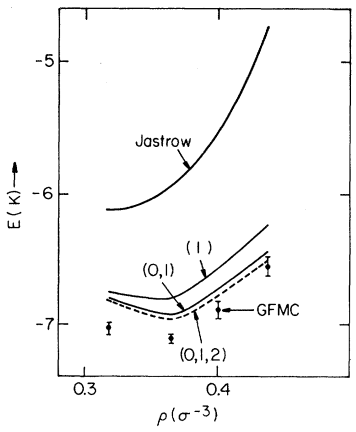

FIG. 5. $E(\rho)$ obtained with Jastrow, $l=1$, $l=0,1$, and $l=0,1,2$ calculations is compared with the GHMC results.

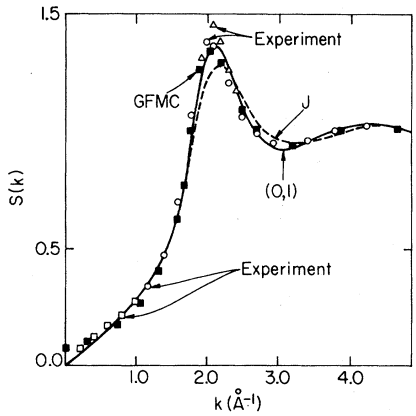

FIG. 6. Static structure function $S(k)$ obtained at $\rho=0.365\sigma^{-3}$ in Jastrow (dashed line), $l=0,1$ (solid line), and GFMC (solid squares) is compared with the experimental data from Refs. 19 (squares), 20 (circles), and 21 (triangles).

The $l=1$ term dominates the q_{ijk} as could be expected on theoretical grounds.[8,9] The $l=0$ correlation appears to have a longer range; $\omega_0>\omega_1$, but it is very weak. The $l=2$ correlation is very small, and has small effects on both $E(\rho)$ and $S(k)$. The calculations were done by successively switching on the $l=1$, 0, and 2 in q_{ijk}. The energy at $\rho=0.365\sigma^{-3}$ is first minimized with respect to variations in λ_1, r_{t1}, and ω_1, then with respect to λ_0, r_{t0}, and ω_0 without varying λ_1, r_{t1}, and ω_1, etc. Thus we did not search for correlations between $l=1$, 0, and 2 components of q_{ijk}. A more detailed search of the variational parameters will need a computational effort that is probably not justified due to the smallness of $l=0$ and 2 correlation. Another improvement in the present variational wave function, over that of Refs. 8 or 9, is in the pair correlation f_{ij}. The optimized f_{ij} used here has the correct long-range behavior needed to obtain the phonon spectrum. Thus it should be useful to study the elementary excitations[4] of liquid ^{4}He with the bare Hamiltonian.

ACKNOWLEDGMENTS

The authors are thankful to Dr. K. E. Schmidt for correspondence and discussions. This work was supported by the NSF under Materials Research Laboratory Grant No. DMR-80-20250 and the U.S. Department of Energy Contract No. DE-AC02-76ER01198.

*On leave from Department of Physics, Aligarh Muslim University, Aligarh, India.
†On leave from Department of Physics, University of Pisa, Pisa, Italy.

[1]P. A. Whitlock, D. M. Ceperley, G. V. Chester, and M. H. Kalos, Phys. Rev. B 19, 5598 (1979).
[2]M. H. Kalos, M. A. Lee, P. A. Whitlock, and G. V. Chester, Phys. Rev. B 24, 115 (1981).
[3]R. A. Aziz, V. P. S. Nain, J. S. Carley, W. L. Taylor, and G. T. McConville, J. Chem. Phys. 70, 4430 (1979).
[4]K. E. Schmidt and V. R. Pandharipande, Phys. Rev. B 20, 3945 (1980).
[5]W. L. McMillan, Phys. Rev. 138, 442 (1965).
[6]M. H. Kalos, D. Levseque, and L. Verlet, Phys. Rev. A 9, 2178 (1974).
[7]C. C. Chang and C. E. Campbell, Phys. Rev. B 15, 4238 (1977).
[8]V. R. Pandharipande, Phys. Rev. B 18, 218 (1978).
[9]K. Schmidt, M. H. Kalos, M. A. Lee, and G. V. Chester, Phys. Rev. Lett. 45, 573 (1980).
[10]R. P. Feynman and M. Cohen, Phys. Rev. 102, 1189 (1956).
[11]Q. N. Usmani, B. Friedman, and V. R. Pandharipande, Phys. Rev. B 25, 4502 (1982).
[12]H. J. Jackson and E. Feenberg, Ann. Phys. (N.Y.) 15, 266 (1961).
[13]V. R. Pandharipande and H. A. Bethe, Phys. Rev. C 7, 1312 (1973).
[14]R. Abe, Prog. Theor. Phys. 21, 421 (1959).
[15]R. A. Smith, A. Kallio, M. Puoskari, and P. Toropainen, Nucl. Phys. A 328, 186 (1979).
[16]R. Alrichs, P. Penco, and G. Scoles, Chem. Phys. 19, 119 (1976).
[17]D. R. McLaughlin and H. F. Schaefer, Chem. Phys. Lett. 12, 244 (1971).
[18]K. Schmidt (private communication).
[19]R. B. Hallock, Phys. Rev. A 5, 320 (1972).
[20]E. C. Svensson, V. F. Sears, A. B. D. Woods, and P. Martel, Phys. Rev. B 21, (1980).
[21]H. N. Robkoff and R. B. Hallock (unpublished).